Category assignment

Article

Short title

In-depth characterization of H_2O_2 sensor in *E. coli*

Title

In-depth characterization of the fluorescent signal of HyPer, a probe for hydrogen peroxide, in bacteria exposed to external oxidative stress

Authors

Joseph B. Lim[1], Kimberly A. Barker[2], Beijing K. Huang[3], Hadley D. Sikes[1*]

[*] indicates corresponding author

Author affiliations

[1]Department of Chemical Engineering, [2]Department of Biology, [3]Department of Biological Engineering, Massachusetts Institute of Technology, 77 Massachusetts Avenue, Building E19-502C, Cambridge, MA 02139 USA

*Department of Chemical Engineering
Massachusetts Institute of Technology
77 Massachusetts Avenue, Building E19-502C, Cambridge, MA 02139 USA
Phone: (+1) 617-253-5224
Fax: (+1) 617-253-2272
Email: sikes@mit.edu

Highlights

- We characterized the signal of HyPer, a fluorescent probe for peroxide, in *E. coli*.
- Each strain requires its own specific signal characterization.
- HyPer's signal is reversible rather than real-time.
- Expression of HyPer reduced the rate of peroxide scavenging by the expression host.
- Careful, controlled use of HyPer facilitates quantitative comparisons across studies.

Abstract

Genetically encoded, fluorescent biosensors have been developed to probe the activities of various signaling molecules inside cells ranging from changes in intracellular ion concentrations to dynamics of lipid second messengers. HyPer is a member of this class of biosensors and is the first to dynamically respond to hydrogen peroxide (H_2O_2), a reactive oxygen species that functions as a signaling molecule. However, detailed characterization of HyPer's signal is not currently available within the context of bacteria exposed to external oxidative stress, which occurs in the immunological response of higher organisms against invasive pathogenic bacteria. Here, we performed this characterization, specifically in *Escherichia coli* exposed to external H_2O_2. We found that the temporal behavior of the signal does not correspond exactly to peroxide concentration in the system as a function of time and expression of the sensor decreases the peroxide scavenging activity of the cell. We also determined the effects of cell

number, both before and after normalization of externally added H_2O_2 to the number of cells. Finally, we report quantitative characteristics of HyPer's signal in this context, including the dynamic range of the signal, the signal-to-noise ratio, and the half saturation constant. These parameters show statistically meaningful differences in signal between two commonly used strains of *E. coli*, demonstrating how signal can vary with strain. Taken together, our results establish a systematic, quantitative framework for researchers seeking to better understand the role of H_2O_2 in the immunological response against bacteria, and for understanding potential differences in the details of HyPer's quantitative performance across studies.

Keywords

Escherichia coli, hydrogen peroxide, HyPer, reactive oxygen species, quantitative redox biology

1. Introduction

Genetically-encoded fluorescent biosensors have been developed to observe and measure many different signaling molecules inside cells [1], including the ions zinc and calcium [2], cyclic adenophosphate [3,4], and lipid second messengers [5], among others. Such sensors rely on conformational changes in a sensor domain induced by the analyte, which then causes a shift in the attached green fluorescent protein family member(s) that can be monitored using spectroscopy. If the binding interaction between the sensor and analyte is reversible or if the sensor is regenerated following a chemical reaction with the analyte, researchers may view and study the dynamics of different signaling processes inside cells.

HyPer is the first genetically-encoded sensor to respond to changes in concentration of hydrogen peroxide (H_2O_2) [6], a reactive oxygen species (ROS) involved in inflammation, immunological responses, and signaling that leads to proliferation and apoptosis in higher organisms [7–11] . The sensor is derived from circularly permuted yellow fluorescent protein and OxyR, an *E. coli* transcription factor that reacts with H_2O_2 with high specificity. H_2O_2 oxidizes one of two key Cys residues, after which the two Cys residues form a disulfide bond [6]. This last step occurs with a conformational change, whereupon cpYFP exhibits an increase in the excitation spectral feature at 500 nm and a decrease at 420 nm (F500 and F420, respectively) when emission is monitored at 530 nm; thus, the ratiometric signal can be correlated with the amount of H_2O_2 present.

Fluorescent dyes such as derivatives of dichlorofluorescein previously used to measure H_2O_2 and other ROS suffer from lack of specificity and artifacts in the signal due to generation of ROS by the dyes themselves when oxidized [12–14]; HyPer does not suffer from these limitations, is genetically encoded and ratiometric, and can be returned to its reduced state by cellular disulfide reductase activity. Because of its numerous advantageous properties, HyPer holds promise for understanding the biological roles of H_2O_2, and its signal has been characterized to an extent and used in many different contexts [15–21].

However, little work has been performed to quantitatively characterize HyPer's fluorescent signal in bacteria when exposed to environmental oxidative stress, which occurs in the immunological response against pathogenic bacteria. While Belousov et al. demonstrated that the spectrum of HyPer expressed in *E. coli* changes as a function of externally added H_2O_2 [6], the behavior of the signal over time in this particular biological context and the effects of assay variables on the signal have yet to be reported. Furthermore, as HyPer's signal in *E. coli* has only been demonstrated by one sample and one spectrum per concentration, the variation of

the signal over the course of multiple biological and technical replicates is not known. Thus, the statistically meaningful quantitative properties of this response, such as the dynamic range of the signal, the signal-to-noise ratio, and the half saturation constant ($K_{1/2}$) have yet to be formally reported. The above characterization would be valuable in showing how HyPer can be used in this biological context in a quantitative manner. This would enhance HyPer's utility in the burgeoning field of quantitative redox biology [22] and the potential development of mathematical models of redox biology in bacteria.

In this study, we highlight the extent to which HyPer may be considered a real-time sensor of H_2O_2 in the context of bacteria and its effects on the cell's ability to scavenge H_2O_2. We ask how the choice of several variables that the researcher controls during the development of an assay impacts HyPer's signal and whether the response varies with cell strain. Finally, we examine the performance of the sensor with biological and technical replicates to draw statistically meaningful conclusions about its analytical capabilities.

2. Materials and methods

2.1. Expression of HyPer

A recombinant pQE30 plasmid containing the HyPer construct was obtained from Evrogen. *E. coli* BL21(DE3) and DH5α cells were transformed with the recombinant HyPer plasmid via electroporation. To express the protein in a bacterial culture, a single colony was used to inoculate 5 ml of Luria-Bertani medium (Becton Dickinson) in a 14 ml culture tube (17 x 100 mm, VWR) and incubated at 37 °C with orbital shaking of 250 rpm overnight. This overnight culture was then used to inoculate 50 ml of Terrific Broth medium (Becton Dickinson) in a non-baffled 250 ml Erlenmeyer flask (VWR) and incubated at 37 °C with orbital shaking of 250 rpm. When cultures reached an OD_{600} of 0.6, cytoplasmic recombinant protein expression was induced by addition of isopropyl β-D-1-thiogalactopyranoside (0.05 mM; Omega Bio-Tek), after which cultures were incubated for 17 hours at 20 °C with orbital shaking of 250 rpm.

2.2. Measurement of HyPer's signal in E. coli over time

After expression of HyPer, cells were centrifuged at 4 °C and 14000 rcf for 5 minutes. The supernatant was discarded and cells were resuspended in Tris buffer (25 mM Tris-HCl obtained from MP Biomedicals, LLC, 150 mM NaCl obtained from Mallinckrodt Pharmaceuticals, pH 8). Cells were washed twice to remove traces of interfering fluorescent components of the growth medium and aliquoted in cell concentrations of 60, 240, and 480 x 10^6 cells per 195 µl based on optical density at 600 nm. A stock solution of H_2O_2 (VWR) was quantified based on absorbance at 240 nm (ε = 43.6 M^{-1} cm^{-1}) and used to prepare serial dilutions of H_2O_2. Cells were added (195 µl) to H_2O_2 (5 µl) in a 96-well microtiter plate (Greiner) to final cell concentrations of 60, 240, and 480 x 10^6 per 200 µl and final H_2O_2 concentrations of 0, 1, 1.5, 2, 2.5, 3, 5, 10, and 20 µM; given the final volume of 200 µl, these concentrations equate to 0, 0.2, 0.3, 0.4, 0.5, 0.6, 1, 2, and 4 nmol. Fluorescence emission intensity was measured upon excitation at 500 nm (9 nm bandwidth) and 420 nm (9 nm bandwidth) with emission monitored at 545 nm (20 nm bandwidth) at 30 second intervals for 20 minutes using a Tecan Infinite M200 plate reader. Measurements were performed at room temperature (~22 °C) and pH 8. To examine whether the kinetics of HyPer's response changed with the availability of an energy source, the above measurement was repeated with the same buffer containing glucose for HyPer expressed in DH5α at a cell density of 60 x 10^6 per 200 µl in response to 20 µM H_2O_2; all conditions were identical except for addition of D-glucose (25 mM, Macron Fine Chemicals) to the assay buffer.

With or without glucose, measurements of the signal showed that both F500 and F420 increased over time, even when no H_2O_2 was exogenously added to the cell suspension (Figures S1 and S2). Both spectral features should in principle remain unchanged when no H_2O_2 is introduced; additionally, the cell suspensions used to measure different amounts of H_2O_2 (0-4 nmol/60 x 10^6 cells) were all taken from the same aliquot of cells. Thus, the increases in F500 and F420 with no exogenous H_2O_2 were subtracted from the time-course plots for F500 and F420 measured with non-zero amounts of exogenously added H_2O_2; all F500/F420 time-course plots were then derived after this treatment of the data.

2.3. Kinetics of H_2O_2 scavenging

Rates of removal of H_2O_2 from solution by DH5α, DH5α expressing HyPer, and BL21(DE3) expressing HyPer were measured using a horseradish peroxidase assay. Cells were washed twice in Tris-glucose buffer (25 mM Tris-HCl obtained from MP Biomedicals, LLC, 150 mM NaCl obtained from Mallinckrodt Pharmaceuticals, 25 mM D-glucose obtained from Macron Fine Chemicals, pH 8) in the manner described in section 2.2. Glucose was added to this resuspension buffer to ensure regeneration of antioxidants such as catalase and alkyl hydroperoxide reductase [23].

For experimental reactions, cells were added (195 µl) to H_2O_2 (5 µl) to a final cell concentration of 60 x 10^6 per 200 µl and a final H_2O_2 concentration of 20 µM (4 nmol). In another set of solutions to determine a standard curve, final H_2O_2 concentrations of 20, 16, 12, 8, 4, and 0 µM were prepared in a volume of 200 µl; these concentrations equate to 4, 3.2, 2.4, 1.6, 0.8, and 0 nmol, respectively.

To quench the experimental reactions at certain time points, 10 µl of hydrochloric acid (HCl, 5 N; Mallinckrodt Pharmaceuticals) was added to a sample containing cells at 2, 4, 6, 8, and 10 minutes. 10 µl of HCl was also added to each standard curve reaction. All samples, both experimental reactions and standard curve reactions, were centrifuged at 4 °C and 14000 rcf for 10 minutes. 160 µl of the supernatant of each sample was added to a 96-well microtiter plate (Greiner). 50 µl of potassium phosphate buffer (1 M, pH 8; VWR) was added to each sample in the plate, followed by 50 µl of 2,2'-azino-bis(3-ethylbenzothiazoline-6-sulphonic acid) (ABTS, 2.5 mM; Tokyo Chemical Industry, Co., Ltd.) in potassium phosphate (0.1 M, pH 8, composed of monopotassium phosphate and dipotassium phosphate obtained from VWR). 10 µl of horseradish peroxidase (HRP, 3 mg/ml; Thermo Scientific) in potassium phosphate (0.1 M, pH 8) was then added. All samples were mixed and the absorbance at 405 nm was measured using a Tecan Infinite M200 plate reader. All samples were repeated twice for a total of three technical replicates for each time point in the experimental runs and each concentration in the standard curve solutions.

The absorbances of the standard curve reactions, i.e. samples without cells were plotted against the final concentrations of H_2O_2 in those samples (Figure S5). Linear least squares regression was performed using Origin software; this calibration was used to determine H_2O_2 amounts in the experimental reactions, i.e. samples containing cells at each time point. Origin software was used to fit a model of exponential decay to the data for each strain to calculate the rate constant for H_2O_2 scavenging (section 2.5).

Two separate biological replicates (independent cultures) were analyzed by repeating the above described measurements, both standard curve reactions and experimental reactions at all time points, for a total of N=6 for each strain.

2.4. Measurement of HyPer's spectrum in E. coli at selected time points

To reduce the parameter space, HyPer's signal was determined at single, selected time points (Table S1) by measuring spectra at 5 nm intervals from 400 to 510 nm, with emission at 545 nm. The measurement was repeated for three total trials at the same experimental conditions used to measure the signal over time (section 2.2) except only at the aforementioned selected time points. The resulting dose-response curves were characterized by using Origin software (Origin Labs) to fit the Hill equation to the curves (section 2.5). The dynamic range was calculated by dividing the maximum ratiometric signal F500/F420 by the signal with no exogenous H_2O_2 added, i.e. the signal at basal levels of H_2O_2 ($F500/F420_{basal}$). The signal-to-noise ratio was calculated by dividing the maximum ratiometric signal by the standard deviation of $F500/F420_{basal}$.

2.5. Statistical analysis

Each data point in the dose-response curves and time-course plots of H_2O_2 scavenging represents mean ± standard deviation of replicate trials.

Origin software was used to fit the following exponential decay function to time-course plots of H_2O_2 scavenging:

$$[nmol\ H_2O_2\ per\ 60{\times}10^6\ cells] = [initial\ nmol\ H_2O_2\ per\ 60{\times}10^6\ cells]e^{-at}$$

where *t* is time in minutes and *a* is the time constant of H_2O_2 decay in min^{-1}. Origin software was also used to fit the following Hill equation to dose-response curves:

$$\frac{F500}{F420} = \frac{F500}{F420_{basal}} + \left(\frac{F500}{F420_{max}} - \frac{F500}{F420_{basal}}\right)\frac{[nmol\ H_2O_2\ per\ 60{\times}10^6\ cells]^n}{K_{1/2} + [nmol\ H_2O_2\ per\ 60{\times}10^6\ cells]^n}$$

where $F500/F420_{max}$ is the maximum signal upon saturation of the sensor, *n* is the Hill coefficient, and $K_{1/2}$ is the half saturation constant, i.e. the amount of H_2O_2 per 60 x 10^6 cells when signal reaches half of its maximum.

All parameters determined by Origin in the fitting of the Hill equation and exponential decay are reported as the calculated parameter ± standard error. To determine the statistical significance of any discrepancies, two-tailed Student's t-tests were used to compare H_2O_2 scavenging time constants between the strains (Table S2), as well as the time constants for the same strain between the two different trials (Table S3). Two-tailed Welch's t-tests were used to compare measured data points in the dose-response curves (Tables S4 to S11). Finally, two-tailed Student's t-tests were used to compare parameters from the Hill equation for each strain measured at 60 x 10^6 cells (Table S12).

3. Results and discussion

HyPer's signal in the cytoplasm of *E. coli* in response to exogenously added H_2O_2 was measured for BL21(DE3) and DH5α. For each strain, cell numbers of 60, 240, and 480 x 10^6 were tested to determine the impact of cell density on the signal. Each combination of strain and cell number was incubated with different amounts of H_2O_2, and the ratiometric signal (F500/F420) was measured both over time (section 2.2) and at selected time points to reduce the parameter space (section 2.3 and Table S1).

We report HyPer's signal in two ways common among users of the probe: the raw ratio F500/F420 and the fold change. Fold change is calculated by dividing the ratio F500/F420 measured in response to a non-zero amount of H_2O_2 by the raw ratio $F500/F420_{basal}$, i.e. the ratio for which no exogenous H_2O_2 was added.

3.1. Temporal behavior of HyPer's signal

HyPer's signal was measured over time after an exogenous addition of hydrogen peroxide (Figure 1). On the basis of existing literature, we expected the ratio F500/F420 to reach a peak value and then decay toward the initial ratio. Figure 1 shows that the rise and decay time scales are not identical for every condition examined. For most combinations of cell number and peroxide amount (Figures 1a,b,c,e) the rise and decay were captured. However, in Figure 1d, the curves for the two highest peroxide concentrations did not decay on the time scale of the experiment, and in Figure 1f, only the tail end of the decay was captured. The rise and peak for this set of conditions likely occurred on a faster time scale than was accessible for these spectroscopic readings. Figure 1 demonstrates that the kinetics of HyPer's response are complex and non-linear in some regimes when the number of cells and the amount of peroxide are varied. Figure S3 shows that for BL21(DE3) measured at 60 x 10^6 cells and DH5α measured at 240 x 10^6 cells, as the amount of H_2O_2 increased, the time required to reach a peak response increased. As a consequence of the observation that the signal can peak at different times in response to the addition of different H_2O_2 amounts, the dose-response curve can evolve over time (Figure S4); hence, the quantification of H_2O_2 depends heavily in some cases upon the timing of the measurement.

Figure 1 (double column)

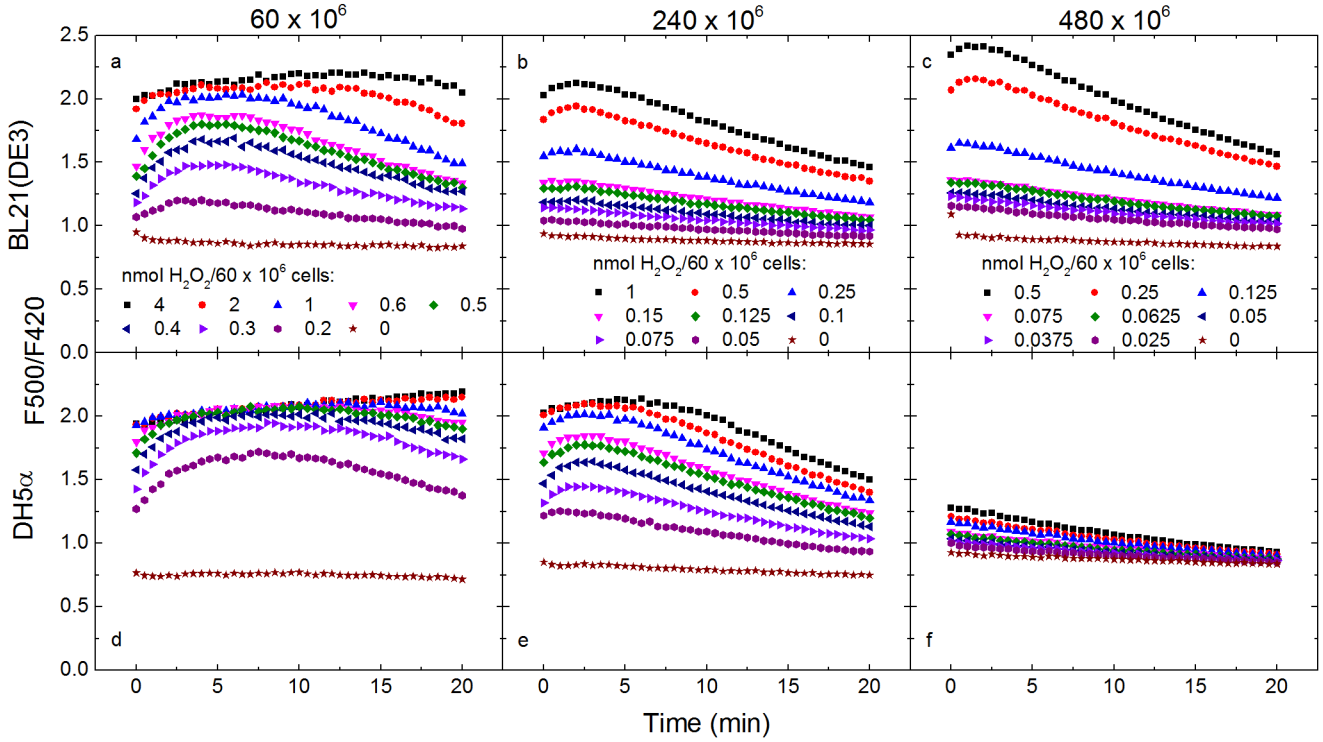

Figure 1. Time-course plots of F500/F420 at cell numbers of 60 (a, d), 240 (b, e), and 480 x 10^6 (c, f) per 200 uL for BL21(DE3) (a, b, c) and DH5α (d, e, f).

To examine the extents to which HyPer acts as a real-time sensor of H_2O_2 concentration and perturbs the H_2O_2 scavenging capacity of the cell, an additional measurement technique was used to measure the concentration of H_2O_2 as a function of time in the cell suspension. BL21(DE3) and DH5α expressing HyPer and DH5α without HyPer were incubated with H_2O_2. The scavenging of H_2O_2 by cells was then stopped via acidification of the entire solution using HCl at different time points, and the amount of remaining H_2O_2 was measured using an HRP/ABTS assay (Figures 2 and S6). 60 x 10^6 cells were used for this measurement because the scavenging rate for this number of cells was slow enough for several time points to be assayed. Higher scavenging rates are expected for cell numbers of 240 and 480 x 10^6. The kinetic measurements of HyPer's signal in BL21(DE3) and DH5α at 60 x 10^6 cells were repeated as described in section 3.1 in buffer supplemented with glucose to compare the temporal behavior of HyPer's signal with the rate at which external H_2O_2 is scavenged by cells.

The data show that the behavior of HyPer's signal as a function of time differs significantly from the exponential decay of peroxide concentration after bolus, exogenous addition indicated by the ABTS signal. This temporal behavior is due to HyPer's reliance on oxidation and reduction of two key Cys residues to exhibit its signal. The oxidation reaction competes with scavenging by antioxidants such as catalase and alkyl hydroperoxide reductase [23]. After oxidation, slow reduction of HyPer due to disulfide reductase activity within the cell occurs, which leads to eventual decreases in the signal (Figure 1). The observation that oxidation occurs more rapidly than reduction is consistent with previous characterization of HyPer's signal in mammalian cells [24,25]. Because of its mechanism of action, HyPer can function as an intracellular, reversible sensor, but researchers should note that its signal reverses well after peroxide has been removed from the system by cellular antioxidants. We also note that HyPer's signal was elevated when measured with glucose present in the assay buffer, with the basal signal and the signal at 4 nmol H_2O_2/60 x 10^6 cells each increased by 2-3 fold; buffer composition is thus another assay variable that must be carefully controlled in measurements of HyPer's signal.

Figure 2 (single column)

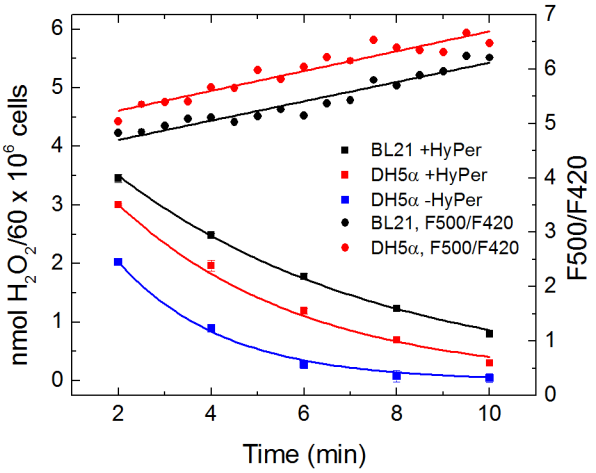

Figure 2. Time-course plots of H_2O_2 scavenging (squares) and F500/F420 (circles) measured at cell number of 60 x 10^6. An absorbance-based horseradish peroxidase assay was used to measure peroxide concentration in solution as a function of time for an initial 20 μM addition of H_2O_2 (4 nmol). Absorbance values were converted to amounts of peroxide using a standard curve (Figure S5). F500/F420 signal is shown in response to this same exogenous addition on the y-axis on the right. Data shown from 2 to 10 minutes.

The calculated H_2O_2 scavenging rate constants are shown in Table 1. Two separate biological replicates were performed to determine culture-to-culture variability of H_2O_2 scavenging by *E. coli* (Figure S6). While BL21(DE3) and DH5α without HyPer exhibited H_2O_2 scavenging rate constants that were consistent between the two separate trials, DH5α with HyPer had two statistically different rate constants (Table S2). In both trials, the scavenging rate constant of each strain was statistically different from the other two (Table S3), with BL21(DE3) being the slowest, followed by DH5α, and then DH5α without HyPer (Table 1). Although HyPer could be considered a scavenger because of its reaction with H_2O_2, its expression in *E. coli* results in decreased overall peroxide scavenging activity, as DH5α without HyPer exhibited higher H_2O_2 scavenging rate constants than DH5α with HyPer in both trials. Given the effects of HyPer expression on H_2O_2 scavenging, the difference in rate constant between the two different trials for DH5α with HyPer but lack of any significant difference for BL21(DE3) suggests that HyPer expression has more variability in DH5α than in BL21(DE3).

Table 1. H_2O_2 scavenging rate constants (min^{-1}) for each strain in each trial.

Strain	BL21(DE3) +HyPer	DH5α +HyPer	DH5α -HyPer
Trial #1	0.17 ± 0.003	0.25 ± 0.01	0.44 ± 0.02
Trial #2	0.17 ± 0.01	0.34 ± 0.02	0.42 ± 0.02

Overall, timing of the measurement clearly has an impact on the dose-response curve developed due to the kinetics of HyPer's signal. Furthermore, HyPer appears to significantly perturb the cell's scavenging capacity; this effect should also be taken into account when integrating HyPer's signal into a quantitative model of redox biology. Dose-response curves were measured at selected time points (Table S1) to further investigate the effects of two other assay variables (cell number and cell strain) and also capture statistically meaningful parameters that quantitatively characterize HyPer's signal, as discussed in sections 3.2 and 3.3.

3.2. Effects of cell number on dose-response curves

Dose-response curves often correlate the signal from cells expressing HyPer with the molar concentration of H_2O_2 added to the cell suspension, as shown in the left-hand panels of Figure 3. The right-hand panels of Figure 3 show the same data in the left-hand panels but correlate the signal with the amount of H_2O_2 per number of cells, rather than the concentration of H_2O_2 of the entire system. The left-hand panels would suggest that the signal, when calculated by either the raw ratio (Figures 3a and 3e) or the fold change (Figures 3c and 3g), has different dynamic ranges at different cell numbers. However, when accounting for the number of cells in the right-hand panels, the signal across different cell numbers collapses such that the dose-response curves for different cell numbers tend to more closely match for both strains at higher amounts of H_2O_2 as evidenced by two-tailed Welch's t-tests (Tables S4 to S11).

Figure 3 (double column)

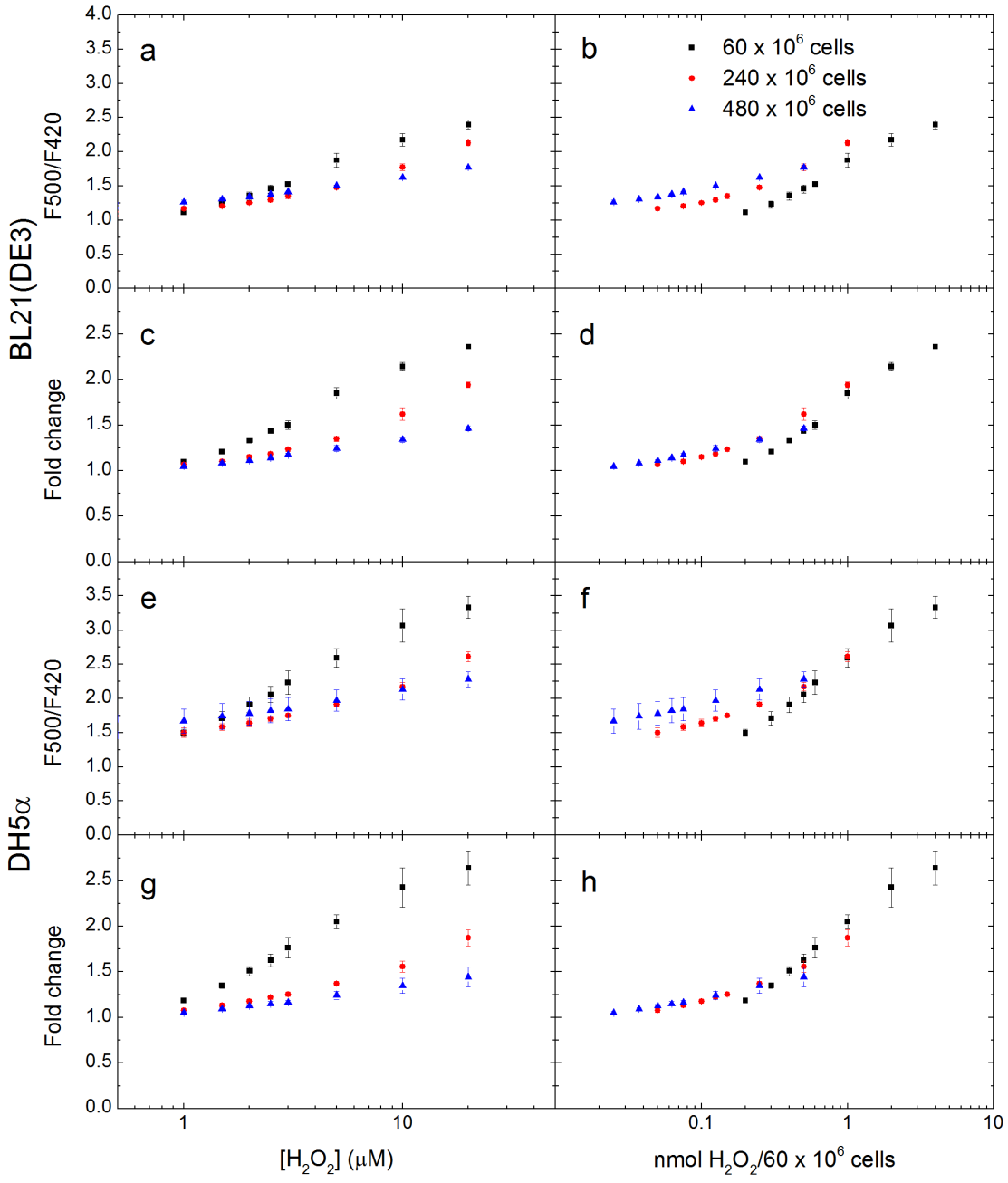

Figure 3. Dose-response curves of F500/F420 or fold change vs [H_2O_2] or H_2O_2 amount normalized to number of cells in assay solution. [H_2O_2] is concentration of the entire assay solution. Curves for both strains (BL21(DE3) and DH5α) at three different cell numbers (60, 240, and 480 x 10^6) are shown. F500/F420 is shown for BL21(DE3) (a, b) and DH5α (e, f). Fold change is also shown for BL21(DE3) (c, d) and DH5α (g, h).

It should be noted that even though the amount of exogenously added H_2O_2 is normalized to the number of cells in the right-hand panels of Figure 3, some slight differences in the signal still persist across different cell numbers. However, these differences do not show different dynamic ranges as in the left-hand panels; rather, the differences lie in the fact that the raw ratio increases with the number of *E. coli* at lower amounts of H_2O_2, even when no H_2O_2 is added ($F500/F420_{basal}$). Given that measurements at all cell numbers were performed on cells taken from the same solution, the increase in signal for higher cell numbers may be due to light scattering by *E. coli*; Kiefer et al., for instance, showed that the absorbance at 500 nm increases more than at 420 nm when the number of cells in solution is increased from 70 x 10^6 to 700 x 10^6 [26]. Thus, it is quite feasible that increases in cell number from 60 x 10^6 to 240 x 10^6 and then to 480 x 10^6 may lead to greater increases in scattering at 500 nm than at 420 nm, which would explain why $F500/F420_{basal}$ and other raw ratios at low H_2O_2 levels generally increase with cell number. The use of fold change to measure the signal takes this variation in raw ratio across different cell numbers into account and effectively eliminates statistically significant differences in the signal (Tables S7 and S11). Thus, while the raw ratio may vary with cell number at particularly low levels of H_2O_2 likely due to light scattering, the fold change can be used to somewhat account for this variation.

The differences in dose-response curve behavior between the left-hand and right-hand panels of Figure 3 demonstrate the importance of controlling the number of cells when measuring HyPer's signal in response to oxidative stress. Given a fixed number of cells and fixed amount of externally added H_2O_2, each cell is exposed to a fraction of the H_2O_2; thus, HyPer exhibits a signal within the cell in response to this fraction of the H_2O_2. Therefore, the amount of H_2O_2 added when measuring HyPer's signal should, in principle, be normalized to the number of cells. Furthermore, even when the number of cells is accounted for in measurement of the signal, light scattering as a function of the number of cells can also impact the raw ratio, particularly at relatively low levels of H_2O_2. The amount of H_2O_2 per some fixed number of cells as well as the total number of cells being measured in a given volume are both variables to which dose-response curves can be quite sensitive.

3.3. Effects of expression host strain on dose-response curves and formal quantitative characterization of the signal

The proof-of-concept work by Belousov et al. [6] did not address the question of whether and how the strain of *E. coli* used affects the signal. The difference in the kinetics of H_2O_2 scavenging between the two strains in this study (Figure 2), as well as the apparent differences in the dose-response curves in the right-hand panels of Figure 3, suggest that that the use of HyPer in two different *E. coli* strains does have an effect on the resulting dose-response curve. To further quantify the differences in the signal between the two strains, we focused on the dose-response curves measured using 60 x 10^6 cells and fitted the Hill equation (section 2.5) to the raw ratiometric signal (Figure 4). The parameters quantifying the dose-response curve according to a fit with an unconstrained Hill coefficient are shown in Table 2.

Figure 4 (single column)

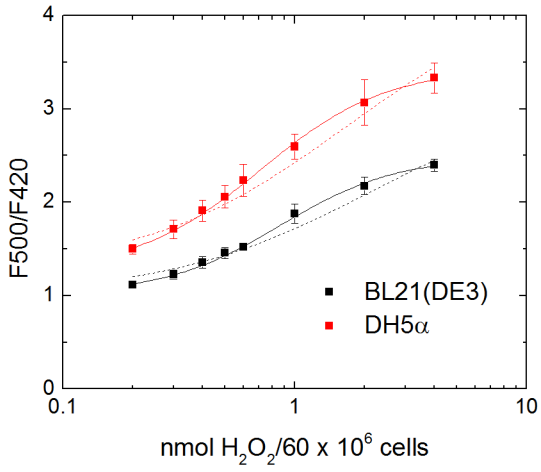

Figure 4. Dose-response curves of F500/F420 vs H_2O_2 amount normalized to number of cells in assay solution. Curves for both strains BL21(DE3) and DH5α at cell number of 60 x 10^6 are shown. The Hill equation was fit to the data, with *n* fixed at 1 (dashed) and not fixed but allowed to be fitted to the data (solid).

Table 2. Quantitative parameters of the fluorescent signal of HyPer in *E. coli* measured at 60 x 10^6 cells.

E. coli strain	BL21(DE3)	DH5α
Dynamic range ($[F500/F420_{max}]/[F500/F420_{basal}]$)	2.45 ± 0.06	2.71 ± 0.11
$K_{1/2}$ (nmol H_2O_2/60 x 10^6 cells)	0.86 ± 0.04	0.71 ± 0.03
Hill coefficient *n*	1.72 ± 0.09	1.62 ± 0.06
Signal-to-noise ratio	120.4	57.2

The dose-response curves in each strain differ in dynamic range, $K_{1/2}$, and signal-to-noise ratio, while the difference in the Hill coefficient *n* is not statistically significant (Table S12). Also notable is that the Hill coefficient *n* is greater than 1 for both strains. This suggests positive cooperativity in the reaction between HyPer and H_2O_2, which in turn suggests that oxidized HyPer may interact in some way with another HyPer molecule that is reduced, facilitating its oxidation by H_2O_2; this would be consistent with the behavior of the OxyR transcription factor [27]. While purified HyPer has been characterized as a monomer, it is also known that it can exist as a mixture of dimers and monomers at higher concentrations [24,25].

The results of assuming the reaction of HyPer with H_2O_2 to be an independent event, fixing *n* at 1, and fitting the Hill equation accordingly are also shown in Figure 4. To fit the equation to the data, the parameter reduced χ^2 was minimized, and was 2.5 and 1.1 for BL21(DE3) and DH5α, respectively, when *n* was fixed at 1; when n was not fixed, the reduced χ^2 was 0.17 and 0.059 for BL21(DE3) and DH5α, respectively, showing that the equation converged to a better fit.

Overall, Figure 4 and Tables 2 and S12 confirm the differences in signal between the two strains suggested by other data in this work. The apparent differences between two different strains of *E. coli* also suggest that other microbes, with possible differences in scavenging

capacity, disulfide reductase activity, and HyPer expression level, may also exhibit different dose-response curves. Thus, dose-response curves should be developed specific to the expression host, without preemptively assuming that a single HyPer molecule reacts with H_2O_2 in an independent fashion.

3.4. Possible factors underlying the differences in HyPer's signal between strains

One possible reason for the difference in HyPer's signal measured in DH5α and BL21(DE3) is the presence of the recA null mutation in the former, which results in as low as 50% cell viability at the time of measurement [28]. While expressed HyPer may still be able to detect H_2O_2 in dead cells, the disulfide reductase machinery is no longer active; thus, HyPer in the oxidized state in dead cells can no longer be reduced to reverse its signal and may also become overoxidized. Because of the recA null mutation, this would be more frequent in the DH5α strain than in BL21(DE3).

Figure 2 clearly showed that the strains also have different scavenging rates, suggesting that they have different expression levels of peroxide scavengers. The primary scavengers in *E. coli* are the catalases KatG and KatE and alkyl hydroperoxide reductase (Ahp) [29]. Ahp is the primary scavenger of endogenously produced H_2O_2 in routine growth conditions [23], while KatE and KatG are better suited for scavenging much higher levels of exogenously introduced H_2O_2 [23]. The scavenging activity of cells containing only Ahp with *katE* and *katG* null mutations, for instance, became saturated at an extracellular H_2O_2 concentration of 20 μM with 45 x 10^6 cells (assuming that an OD_{600} of 1 approximately equates to 10^9 cells/ml) present in a 0.45 ml volume (6.75 nmol H_2O_2/60 x 10^6 cells), and was limited by the availability of NADH. In contrast, the scavenging activity of cells expressing only catalase did not become saturated even in the presence of millimolar concentrations of H_2O_2 [23]. Given the concentrations of H_2O_2 used in our study, it is likely that KatG and KatE were the primary scavengers in our measurements, and possible that the expression levels of these scavengers differ between different strains. KatE, for instance, is induced by the RpoS system [30]; because the level of RpoS can vary between strains and isolates of the same strain, this may result in different expression levels of KatE. The expression levels and thus total activities of the primary scavengers in *E. coli* may vary between strains, which would affect the signal due to potential kinetic competition between scavengers and HyPer for H_2O_2.

We also note that the induction of certain genes in *E. coli* depend on growth conditions. Expression of Ahp and KatG are primarily regulated by the OxyR transcription factor [31], while KatE is strongly expressed only in the stationary phase and induced by the RpoS system [30]. In our experiments, the cultures were grown to stationary phase and introduced to exogenous H_2O_2, meaning that all three scavengers were induced. Thus, a different set of conditions in which HyPer might have been expressed could have changed the expression levels of the primary scavengers and consequently their competition with HyPer and the resulting fluorescent signal. If the cultures had not been grown to stationary phase, for instance, then the KatE catalase could have been removed as a potential contributor to scavenging activity. Because growth conditions affect the expression levels of the primary scavengers, growth conditions are also an important variable to consider when measuring HyPer's signal in cells in response to exogenous H_2O_2.

4. Conclusions

Overall, our study shows the importance of controlling several variables when assaying HyPer's intracellular signal in response to external oxidative stress. The timing of the measurement is important in the generation of a dose-response curve and the resolution it provides, since this curve evolves over time after exposure to oxidative insult. Furthermore, expression of HyPer may reduce the cell's peroxide scavenging capacity; this effect should be taken into account by measuring the scavenging rate both with and without HyPer. The number of cells should also be controlled to allow normalization of the amount of exogenously added H_2O_2 and also to account for variations in the signal due to possible light scattering by the cells themselves, particularly at low levels of H_2O_2 per cell. The expression host used also affects the signal, likely due to differences in scavenging capacity, disulfide reductase activity, HyPer expression, and cell viability. Growth conditions also influence scavenging capacity by affecting which scavengers are expressed and to what levels, making growth conditions for HyPer expression another important variable to control.

We establish a framework for systematically measuring dose-response curves in this physiological context and generating statistically meaningful properties of the response. When the variables mentioned above – timing of measurement, effects of HyPer expression on the cell's scavenging capacity, number of cells, and expression host – are well controlled and accounted for, the parameters obtained from a dose-response curve should facilitate meaningful comparisons of the signal across different studies. This framework should enable reproducible use of HyPer in more quantitative studies of biological processes in which cells are exposed to external oxidative stress.

Acknowledgements

J.B.L. acknowledges support from a National Science Foundation Graduate Research Fellowship. H.D.S. acknowledges support from a Burroughs Wellcome Fund Career Award at the Scientific Interface, the Joseph R. Mares endowed chair in chemical engineering, and the James H. Ferry Fund for Innovation. We thank Joy Lee and Sohail F. Ali for helpful discussions during this work.

References

[1] R.H. Newman, J. Zhang, The design and application of genetically encodable biosensors based on fluorescent proteins, in: J. Zhang, Q. Ni, R.H. Newman (Eds.), Fluoresc. Protein-Based Biosens., Humana Press, Clifton, NJ, 2014: pp. 1–16. doi:10.1007/978-1-62703-622-1_1.

[2] J.G. Park, A.E. Palmer, Quantitative measurement of Ca2+ and Zn2+ in mammalian cells using genetically encoded fluorescent biosensors, in: J. Zhang, Q. Ni, R.H. Newman (Eds.), Fluoresc. Protein-Based Biosens., Humana Press, Clifton, NJ, 2014: pp. 29–47. doi:10.1007/978-1-62703-622-1_3.

[3] J. Klarenbeek, K. Jalink, Detecting cAMP with an EPAC-based FRET sensor in single living cells, in: J. Zhang, Q. Ni, R.H. Newman (Eds.), Fluoresc. Protein-Based Biosens., Humana Press, Clifton, NJ, 2014: pp. 49–58. doi:10.1007/978-1-62703-622-1_4.

[4] A. Stangherlin, A. Koschinski, A. Terrin, A. Zoccarato, H. Jiang, L.A. Fields, et al., Analysis of compartmentalized cAMP: a method to compare signals from differently targeted FRET reporters, in: J. Zhang, N. Qiang, R.H. Newman (Eds.), Fluoresc. Protein-

Based Biosens., Humana Press, Clifton, NJ, 2014: pp. 59–71. doi:10.1007/978-1-62703-622-1_5.

[5] M. Sato, Genetically encoded fluorescent biosensors for live cell imaging of lipid dynamics, in: J. Zhang, N. Qiang, R. Newman (Eds.), Fluoresc. Protein-Based Biosens., Humana Press, Clifton, NJ, 2014: pp. 73–81. doi:10.1007/978-1-62703-622-1_6.

[6] V. V. Belousov, A.F. Fradkov, K.A. Lukyanov, D.B. Staroverov, K.S. Shakhbazov, A. V. Terskikh, et al., Genetically encoded fluorescent indicator for intracellular hydrogen peroxide, Nat. Methods. 3 (2006) 281–6. doi:10.1038/nmeth866.

[7] C.C. Winterbourn, Reconciling the chemistry and biology of reactive oxygen species, Nat. Chem. Biol. 4 (2008) 278–286. doi:10.1038/nchembio.85.

[8] B.C. Dickinson, C.J. Chang, Chemistry and biology of reactive oxygen species in signaling or stress responses, Nat. Chem. Biol. 7 (2011) 504–11. doi:10.1038/nchembio.607.

[9] M.L. Circu, T.Y. Aw, Reactive oxygen species, cellular redox systems, and apoptosis, Free Radic. Biol. Med. 48 (2010) 749–62. doi:10.1016/j.freeradbiomed.2009.12.022.

[10] B. Halliwell, J. Gutteridge, Free Radicals in Biology and Medicine, Fourth, Oxford University Press, New York, 2007.

[11] B. D'Autréaux, M.B. Toledano, ROS as signalling molecules: mechanisms that generate specificity in ROS homeostasis, Nat. Rev. Mol. Cell Biol. 8 (2007) 813–24. doi:10.1038/nrm2256.

[12] J.P. Crow, Dichlorodihydrofluorescein and dihydrorhodamine 123 are sensitive indicators of peroxynitrite in vitro: implications for intracellular measurement of reactive nitrogen and oxygen species, Nitric Oxide Biol. Chem. 1 (1997) 145–57. doi:10.1006/niox.1996.0113.

[13] E. Marchesi, C. Rota, Y.C. Fann, C.F. Chignell, R.P. Mason, Photoreduction of the fluorescent dye 2′-7′-dichlorofluorescein: a spin trapping and direct electron spin resonance study with implications for oxidative stress measurements, Free Radic. Biol. Med. 26 (1999) 148–161. doi:10.1016/S0891-5849(98)00174-9.

[14] C. Rota, Y.C. Fann, R.P. Mason, Phenoxyl Free Radical Formation during the Oxidation of the Fluorescent Dye 2',7'-Dichlorofluorescein by Horseradish Peroxidase: Possible Consequences for Oxidative Stress Measurements, J. Biol. Chem. 274 (1999) 28161–28168. doi:10.1074/jbc.274.40.28161.

[15] A. Hernández-Barrera, C. Quinto, E.A. Johnson, H.-M. Wu, A.Y. Cheung, L. Cárdenas, Using hyper as a molecular probe to visualize hydrogen peroxide in living plant cells: a method with virtually unlimited potential in plant biology, Methods Enzymol. 527 (2013) 275–90. doi:10.1016/B978-0-12-405882-8.00015-5.

[16] P. Niethammer, C. Grabher, A.T. Look, T.J. Mitchison, A tissue-scale gradient of hydrogen peroxide mediates rapid wound detection in zebrafish, Nature. 459 (2009) 996–9. doi:10.1038/nature08119.

[17] J.L. Sartoretto, H. Kalwa, M.D. Pluth, S.J. Lippard, T. Michel, Hydrogen peroxide differentially modulates cardiac myocyte nitric oxide synthesis, Proc. Natl. Acad. Sci. U. S. A. 108 (2011) 15792–7. doi:10.1073/pnas.1111331108.

[18] R. Ameziane-El-Hassani, M. Boufraqech, O. Lagente-Chevallier, U. Weyemi, M. Talbot, D. Métivier, et al., Role of H2O2 in RET/PTC1 chromosomal rearrangement produced by ionizing radiation in human thyroid cells, Cancer Res. 70 (2010) 4123–32. doi:10.1158/0008-5472.CAN-09-4336.

[19] A. Espinosa, A. García, S. Härtel, C. Hidalgo, E. Jaimovich, NADPH oxidase and hydrogen peroxide mediate insulin-induced calcium increase in skeletal muscle cells, J. Biol. Chem. 284 (2009) 2568–75. doi:10.1074/jbc.M804249200.

[20] B.Y. Jin, J.L. Sartoretto, V.N. Gladyshev, T. Michel, Endothelial nitric oxide synthase negatively regulates hydrogen peroxide-stimulated AMP-activated protein kinase in endothelial cells, Proc. Natl. Acad. Sci. U. S. A. 106 (2009) 17343–8. doi:10.1073/pnas.0907409106.

[21] M.P. Brynildsen, J.A. Winkler, C.S. Spina, I.C. Macdonald, J.J. Collins, Potentiating antibacterial activity by predictably enhancing endogenous microbial ROS production, Nat. Biotechnol. 31 (2013) 160–5. doi:10.1038/nbt.2458.

[22] G.R. Buettner, B.A. Wagner, V.G.J. Rodgers, Quantitative Q3 redox biology: an approach to understanding the role of reactive species in defining the cellular redox environment, Cell Biochem. Biophys. 67 (2013) 477–483. doi:10.1007/s12013-011-9320-3.

[23] L.C. Seaver, J.A. Imlay, Alkyl hydroperoxide reductase is the primary scavenger of endogenous hydrogen peroxide in Escherichia coli, J. Bacteriol. 183 (2001) 7173–81. doi:10.1128/JB.183.24.7173-7181.2001.

[24] K.N. Markvicheva, D.S. Bilan, N.M. Mishina, A.Y. Gorokhovatsky, L.M. Vinokurov, S. Lukyanov, et al., A genetically encoded sensor for H2O2 with expanded dynamic range, Bioorg. Med. Chem. 19 (2011) 1079–84. doi:10.1016/j.bmc.2010.07.014.

[25] D.S. Bilan, L. Pase, L. Joosen, A.Y. Gorokhovatsky, Y.G. Ermakova, T.W.J. Gadella, et al., HyPer-3: A Genetically Encoded H(2)O(2) Probe with Improved Performance for Ratiometric and Fluorescence Lifetime Imaging, ACS Chem. Biol. 8 (2013) 535–542. doi:10.1021/cb300625g.

[26] J. Kiefer, N. Ebel, E. Schlücker, A. Leipertz, Characterization of Escherichia coli suspensions using UV/Vis/NIR absorption spectroscopy, Anal. Methods. 2 (2010) 123–128. doi:10.1039/b9ay00185a.

[27] C. Lee, S.M. Lee, P. Mukhopadhyay, S.J. Kim, S.C. Lee, W.-S. Ahn, et al., Redox regulation of OxyR requires specific disulfide bond formation involving a rapid kinetic reaction path, Nat. Struct. Mol. Biol. 11 (2004) 1179–85. doi:10.1038/nsmb856.

[28] F. Capaldo-Kimball, S.D. Barbour, Involvement of Recombination Genes in Growth and Viability of Escherichia coli K-12, J. Bacteriol. 106 (1971) 204–212.

[29] J.A. Imlay, The molecular mechanisms and physiological consequences of oxidative stress: lessons from a model bacterium, Nat. Rev. Microbiol. 11 (2013) 443–54. doi:10.1038/nrmicro3032.

[30] H.E. Schellhorn, H.M. Hassan, Transcriptional regulation of katE in Escherichia coli K-12, J. Bacteriol. 170 (1988) 4286–4292.

[31] M.F. Christman, G. Storz, B.N. Ames, OxyR, a positive regulator of hydrogen peroxide-inducible genes in Escherichia coli and Salmonella typhimurium, is homologous to a family of bacterial regulatory proteins, Proc. Natl. Acad. Sci. 86 (1989) 3484–3488. doi:10.1073/pnas.86.10.3484.